

Synthesis And Biological Activity of Amide Derivatives Derived From Natural Product Waltherione F

Hongbin Fang

Liaocheng University

Zhanfang Chen

Liaocheng University

Xuwen Hua (✉ huaxuwen906@163.com)

Liaocheng University <https://orcid.org/0000-0002-5748-6473>

Wenrui Liu

Liaocheng University

Chenmeng Xue

Liaocheng University

Yi Liu

Liaocheng University

Xiaohe Zhu

Liaocheng University

Man Yuan

Liaocheng University

Shuang Cheng

Liaocheng University

Bingxiang Wang

Liaocheng University

Jing Ru

Liaocheng University

Dzmitry Bazhanau

Liaocheng University

Yanhong Cui

Zhejiang University of Technology

Research Article

Keywords: Waltherione F, amide compounds, structural optimization, biological activity, fluorescence characteristic

Posted Date: November 23rd, 2021

DOI: <https://doi.org/10.21203/rs.3.rs-1071215/v1>

License:  This work is licensed under a Creative Commons Attribution 4.0 International License.

[Read Full License](#)

Version of Record: A version of this preprint was published at Medicinal Chemistry Research on February 7th, 2022. See the published version at <https://doi.org/10.1007/s00044-022-02852-8>.

Abstract

Structural optimization based on natural products has become an effective way to develop new green fungicides, which provide important guiding significance for practicing the new development concept and promoting the green development of pesticides. In this project, combined with the fungicidal amide lead compound X-I-4 discovered in our previous work and fungicidal piperazine derivatives reported in literatures, the target compounds containing 4-quinolone and piperazine substructures based on waltherione F were designed, synthesized and screened for their biological activity. The bioassay results indicated that compounds I-3, I-5, II-3, II-7, II-10, II-11 and II-13 displayed higher inhibition rates against *Rhizoctonia solani* than other tested compounds. The in vitro cellular cytotoxicity assay revealed the compounds II-6 and II-11 exhibited higher cytotoxicity against HepG2 than other tested compounds. The fluorescence characteristics investigation showed that the absolute fluorescence QY value of the methanol solution of the compound I-6 was higher than those of I-2, I-3, I-7 and I-8, which was further elucidated by TD-DFT.

1 Introduction

Agrochemicals are important production materials for agricultural production, and provide significant material support for modern agricultural development. Fungicides are an important part of agrochemicals, which are related to the safety of national food, vegetables, and fruits, and have occupied nearly 30% of the agrochemical market. However, with the long-term and large-scale use of traditional chemical synthetic fungicides, negative problems such as environmental pollution, pathogen resistance, and poisoning to beneficial insects and microorganisms have become increasingly prominent.^[1, 2] Therefore, the development of efficient, safe, low residual, and environmentally friendly green fungicides has become an inevitable trend for pesticide innovation.^[3, 4]

Natural products have received extensive attention from scientific researchers due to their novel structures, unique mechanism of action, wide sources, no cross-resistance, fast biodegradation, and eco-friendliness. For example, osthol, matrine, berberine, and eugenol have been successfully used in the control of agricultural pathogens.^[5, 6] However, low extraction rate, difficult chemical synthesis, poor environmental stability, and poor biological activity are the problems that natural products face at present.^[7] Developing new green fungicides, which was derived from the structural optimization of natural products, can effectively deal with the problems such as low safety and high pathogen resistance of traditional fungicides, and narrow fungicidal spectrum and short duration of natural products.^[7-11]

Waltherione F is a 4-quinolone alkaloid, which was isolated from *Waltheria indica* L. of the Sterculiaceae family and found to exhibit good antifungal activity.^[12-14] In our previous work, 4-quinolone derivatives **QD** and quinoline derivatives **X-II** derived from natural product waltherione F were synthesized and evaluated for their biological activity, of which compounds **QD-1** and **X-II-5** were discovered to have a good fungicidal activity (Fig. 1).^[15] In this project, combined with the fungicidal amide lead compound **h-I-9** discovered in our previous work and fungicidal piperazine compounds **P-1** and **P-2** reported in

literatures,^[16-21] the amide derivatives containing 4-quinolone and piperazine substructures were designed, prepared and screened for their biological activity (Fig. 2).

2 Results And Discussion

2.1 Organic synthesis

The corresponding intermediates and amide derivatives **I-1 – I-9**, **II-1 – II-13** containing 4-quinolone group were synthesized in accordance with the procedures displayed in Scheme 1. Firstly, the material 2-methoxy-5-methylaniline was reacted with dimethyl acetylene to prepare the molecule **2**, which was cyclized to give ester **3** by using polyphosphoric acid (PPA) as the condensing reagent to perform the Conrad-Limpach reaction. The carboxylic acid **4** was obtained by hydrolyzing the ester group with lithium hydroxide. Subsequently, the target molecules **I-1 – I-9** were synthesized by the condensation reaction between the carboxylic acid **4** and substituted amines with HATU/DIEA as the condensing agent. In the preparation of the target molecules **II-1 – II-13**, the intermediate **5** was produced by the condensation reaction of the carboxylic acid **4** and *tert*-butyl piperazine-1-carboxylate with TBTU/DIEA as the condensing agent, and then further deprotected with trifluoroacetic acid to provide the amide derivative **6**. Finally, the substituted carboxylic acid was reacted, respectively, with intermediate **6** to gain the target molecules **II-1 – II-13** using EDCI/HOBt as the condensing reagent. Subsequently, the obtained structures were characterized with ¹H NMR, ¹³C NMR and HRMS. In view of the melting points of the target molecules, and combined with the TLC monitoring results, the target molecules exhibited the characteristics of strong polarity. In addition, the crystal of compound **I-6** was cultivated from methanol and DCM, and determined on a Bruker D8 Venture diffractometer to provide several structural characteristics (Fig. 3, CCDC Number 2112787).

2.2 Fungicidal activity and in vitro cellular cytotoxicity

The in vitro inhibitory activities of the target molecules against the common agricultural pathogens was investigated, and the results are shown in Table 1. From the data, the compounds **I-1 – I-9** and **II-1 – II-13** showed weak fungicidal activity against the tested agricultural pathogens, which may be related to the strong polarity of the compounds. However, in a given category, several compounds displayed higher inhibition rates against the specific tested pathogens than other compounds. For example, the compounds **I-3**, **I-5**, **II-3**, **II-7**, **II-11** and **II-13** exhibited better fungicidal activity against *Rhizoctonia solani* than other compounds. Moreover, the compounds **I-8** and **II-6** showed better fungicidal activity against *Colletotrichum capsici* than other compounds. From the perspective of structural characteristics, there was no significant difference in fungicidal activity between **I-1 – I-9** and **II-1 – II-13**. Considering the antitumor activity of waltherione F reported in literatures, the in vitro cellular cytotoxicity assay of the target compounds against HepG2 at 100 μM was performed, and the results was shown in Table2. From the data, it could be observed that the compounds **I-1 – I-9** and **II-1 – II-13** showed weak antitumor activity

against HepG2. However, the compounds **II-6** and **II-11** exhibited higher cytotoxicity than other tested compounds.

Table 1
The in vitro inhibitory activity of the target compounds at 100 µmol/L

Compounds	Inhibition rate/%							
	GZ	RS	CS	AK	PP	BC	CC	AS
I-1	7.9 ± 0.62	1.3 ± 0.45	21.5 ± 0.61	1.8 ± 0.23	3.7 ± 0.34	5.5 ± 0.34	0.6 ±0.44	9.5 ± 0.61
I-2	1.9 ± 0.47	0.2 ± 0.52	17.2 ± 0.57	7.9 ± 0.27	2.2 ± 0.24	11.9 ± 0.36	1.0 ± 0.38	9.9 ± 0.64
I-3	7.8 ± 0.33	38.0 ± 0.22	24.1 ± 0.59	16.6 ± 0.27	8.0 ± 0.25	5.4 ± 0.31	2.7 ± 0.67	13.9 ± 0.75
I-4	11.5 ± 0.52	0.8 ± 0.52	24.7 ± 0.78	21.8 ± 0.23	7.1 ± 0.34	14.8 ± 0.36	19.5 ± 0.33	13.2 ± 0.71
I-5	7.9 ± 0.40	44.0 ± 0.33	16.7 ± 0.61	12.8 ± 0.27	15.1 ± 0.20	12.1 ± 0.49	26.3 ± 0.38	13.8 ± 0.33
I-6	14.4 ± 0.33	26.1 ± 0.43	12.6 ± 0.57	13.3 ± 0.28	12.2 ± 0.20	3.3 ± 0.43	26.5 ± 0.46	8.6 ± 0.43
I-7	11.3 ± 0.33	2.2 ± 0.32	17.3 ± 0.50	7.3 ± 0.16	1.9 ± 0.23	14.9 ± 0.29	0.9 ± 0.44	11.5 ± 0.59
I-8	14.1 ± 0.59	1.1 ± 0.59	21.1 ± 0.49	14.5 ± 0.28	1.2 ± 0.17	6.8 ± 0.27	37.4 ± 0.36	19.3 ± 0.77
I-9	11.2 ± 0.62	1.1 ± 0.33	20.1 ± 0.78	7.0 ± 0.32	7.4 ± 0.29	19.7 ± 0.73	1.2 ± 0.44	17.3 ± 0.61
II-1	17.4 ± 0.55	1.1 ± 0.48	16.9 ± 0.43	3.3 ± 0.41	5.8 ± 0.45	11.6 ± 0.29	1.0 ± 0.46	10.3 ± 0.75
II-2	18.7 ± 0.84	0.9 ± 0.47	25.0 ± 0.61	14.2 ± 0.27	13.8 ± 0.23	12.8 ± 0.36	27.0 ± 0.38	5.3 ± 0.51
II-3	12.0 ± 0.55	37.5 ± 0.45	17.2 ± 0.68	18.0 ± 0.35	29.4 ± 0.30	2.7 ± 0.48	16.1 ± 0.46	5.7 ± 0.44
II-4	19.4 ± 0.29	0.7 ± 0.28	16.9 ± 0.57	22.4 ± 0.20	10.3 ± 0.20	8.8 ± 0.42	0.7 ± 0.32	12.0 ± 0.52
II-5	8.3 ± 0.72	12.5 ± 0.33	17.9 ± 0.81	13.6 ±0.22	9.8 ± 0.28	8.4 ± 0.61	23.8 ± 0.43	4.9 ± 0.15
II-6	16.2 ± 0.83	0.6 ± 0.45	26.0 ± 0.68	24.2 ± 0.24	15.3 ± 0.20	14.5 ± 0.43	37.1 ± 0.38	9.2 ± 0.52
II-7	14.6 ± 0.28	37.7 ± 0.38	17.2 ± 0.57	10.9 ± 0.28	11.6 ± 0.34	3.3 ±0.36	21.9 ± 0.38	12.9 ± 0.25
II-8	27.2 ± 0.37	1.7 ± 0.32	13.9 ± 0.29	2.4 ± 0.19	31.2 ± 0.32	11.9 ± 0.31	2.4 ± 0.77	5.6 ± 0.58

Compounds	Inhibition rate/%							
	GZ	RS	CS	AK	PP	BC	CC	AS
II-9	11.5 ± 0.59	0.6 ± 0.37	12.9 ± 0.74	4.9 ± 0.27	2.0 ± 0.19	8.3 ± 0.40	2.5 ± 0.56	4.5 ± 0.45
II-10	4.8 ± 0.37	35.2 ± 0.40	16.7 ± 0.57	9.2 ± 0.22	7.7 ± 0.34	8.6 ± 0.25	30.4 ± 0.38	9.8 ± 0.59
II-11	10.5 ± 0.45	38.3 ± 0.33	16.4 ± 0.44	15.0 ± 0.20	2.3 ± 0.28	3.3 ± 0.17	1.6 ± 0.68	9.5 ± 0.66
II-12	20.8 ± 0.48	1.0 ± 0.47	20.3 ± 0.52	6.6 ± 0.27	1.4 ± 0.23	14.7 ± 0.43	0.6 ± 0.52	12.8 ± 0.45
II-13	11.6 ± 0.33	36.9 ± 0.37	21.1 ± 0.61	15.3 ± 0.18	16.0 ± 0.36	20.5 ± 0.30	21.5 ± 0.44	11.8 ± 0.52
Fluopyram	100	61.5 ± 0.38	100	94.5 ± 0.23	31.8 ± 0.16	60.7 ± 0.48	51.8 ± 0.32	100
Carbendazim	100	100	12.1 ± 0.49	13.3 ± 0.20	100	90.1 ± 0.21	100	7.3 ± 0.51

GZ, *Gibberella zeae*; RS, *Rhizoctonia solani*; CS, *Cercospora circumscissa* Sacc.; AK, *Alternaria kikuchiana* Tanaka; PP, *Physalospora piricola*; BC, *Botrytis cinerea*; CC, *Colletotrichum capsici*; AS, *Alternaria sp.*

Table 2
Cytotoxic profiles of the target compounds against HepG2 at 100 μM

Compounds	Cytotoxicity/%	Compounds	Cytotoxicity/%	Compounds	Cytotoxicity/%
I-1	5.8 ± 0.31	II-1	4.5 ± 1.13	II-10	0
I-2	1.1 ± 1.06	II-2	12.2 ± 0.88	II-11	25.6 ± 2.06
I-3	2.7 ± 0.59	II-3	5.9 ± 0.16	II-12	16.3 ± 1.31
I-4	7.9 ± 1.67	II-4	0	II-13	17.5 ± 0.80
I-5	6.1 ± 1.66	II-5	6.8 ± 1.25		100
I-6	0	II-6	26.2 ± 1.35		
I-7	3.3 ± 0.41	II-7	8.8 ± 1.14		
I-8	0	II-8	13.9 ± 0.94		
I-9	9.5 ± 0.34	II-9	0		

2.3 Fluorescence Characteristic Investigation

Considering the fluorescence characteristics of 4-quinolone derivatives **QD** and quinoline derivatives **X-II** exhibited in our previous work, the UV-vis absorption and fluorescence emission spectra of the

compounds **I-1** – **I-9** and **II-1** – **II-13** were scanned and shown in Fig. 4. From the data, the compounds **I-6** and **I-7** displayed a stronger fluorescence intensity than other compounds. Afterwards, the absolute fluorescence QY values of the methanol solutions (50 μ M) of the compounds **I-2**, **I-3**, **I-6**, **I-7** and **I-8** were measured to further illustrate the fluorescence characteristics, and the results were exhibited in Table 3. It could be found that compound **I-6** exhibited a higher QY than that of **I-2**, **I-3**, **I-7**, and **I-8**, with a value of 27.4%. Subsequently, the TD-DFT calculations of molecules **I-6** and **I-7** were performed to elucidate the obtained fluorescence properties (Fig. 5). From the data, the HOMO orbital energy and LUMO orbital energy of molecule **I-6** were both higher than that of **I-7**, which was conducive to the energy level transitions of electrons in the HOMO orbital of molecule **I-6**. In the meantime, the molecule **I-6** exhibited a larger energy gap than **I-7**, which help **I-6** absorb more energy to produce stronger fluorescence intensity.

Table 3
The absolute fluorescence quantum yields (QY) of compounds **I-2**, **I-3**, **I-6**, **I-7** and **I-8** in methanol

Compounds	QY (%)	Compounds	QY (%)	Compounds	QY (%)
I-2	19.6	I-6	27.4	I-8	11.4
I-3	15.5	I-7	15.5		

3 Conclusion

In summary, twenty-two novel amide derivatives derived from the structural modification of waltherione F were designed and synthesized. The obtained structures were characterized by ^1H NMR, ^{13}C NMR and HRMS. Several crystal structural characteristics were also revealed via X-ray crystal diffraction of compounds **I-6**. The bioassay results indicated that the compounds **I-1** – **I-9** and **II-1** – **II-13** showed weak inhibitory activities against the tested agricultural pathogens. However, in a given category, several compounds displayed higher inhibition rates against *Rhizoctonia solani* than other compounds. The in vitro cellular cytotoxicity assay revealed the compounds **II-6** and **II-11** exhibited higher cytotoxicity against HepG2 than other tested compounds. The fluorescence characteristics investigation showed that the QY value of the methanol solution of the compound **I-6** was higher than that of **I-2**, **I-3**, **I-7** and **I-8**, which was further explained by TD-DFT.

4 Experimental

4.1 Material and instruments

The materials and reagents used in the organic synthesis reactions were of analytical grade, and purchased from Energy Chemical and Bide Pharmatech Ltd. Melting points were measured on an X-5 binocular microscope. ^1H - and ^{13}C - NMR were provided on a Bruker-500 MHz spectrometer. HRMS (Waters Xevo G2-XS QToF, USA) was used to record the relative molecular mass. X-ray crystal structure

was determined on a Bruker D8 Venture diffractometer. The purification of target compounds was performed by the column chromatography on silica gel (200–300 mesh).

4.2 Preparation of the target molecules

4.2.1 Synthetic procedure for I-1–I-9

8-methoxy-5-methyl-4-oxo-*N*-phenyl-1,4-dihydroquinoline-2-carboxamide (**I-1**) was synthesized as follows. To a mixture of 8-methoxy-5-methyl-4-oxo-1,4-dihydroquinoline-2-carboxylic acid (0.50 g, 2.1 mmol), HATU (1.14 g, 3.0 mmol), DIEA (0.66 g, 5.1 mmol) in DMF (10 mL) was added aniline (0.24 g, 2.6 mmol). The solution was reacted for 12h at room temperature, and then poured into DCM (100 mL). The organic phase was washed with water (100 mL), and separated by extraction. The obtained organic layer was dried, filtered and concentrated. The resulting residue was purified by chromatograph on silica gel using DCM/methanol (v/v = 50/1) as eluent to obtain **I-1**. Compounds **I-2** – **I-9** were prepared similarly.

8-methoxy-5-methyl-4-oxo-*N*-phenyl-1,4-dihydroquinoline-2-carboxamide (**I-1**): White solid, yield 56%, m.p. 277–278°C. ¹H NMR (DMSO-*d*₆, 500 MHz) δ 10.69 (1H, s, NH), 9.83 (1H, s, CONH), 7.81 (2H, d, *J* = 7.8 Hz, Ph-H), 7.41 (2H, t, *J* = 7.9 Hz, Ph-H), 7.23 – 7.16 (2H, m, Ph-H), 7.05 – 6.99 (2H, m, quinolone-H and Ph-H), 4.00 (3H, s, OCH₃), 2.73 (3H, s, Ph-CH₃). ¹³C NMR (DMSO-*d*₆, 126 MHz) δ 180.8, 160.5, 146.9, 139.0, 138.3, 131.8, 130.2, 129.3, 125.7, 125.3, 124.4, 121.3, 111.9, 110.0, 56.9, 22.6. HRMS (ESI⁺) *m/z* calcd for C₁₈H₁₇N₂O₃ 309.1234, found 309.1233 [M + H]⁺.

N-(2,3-dichlorophenyl)-8-methoxy-5-methyl-4-oxo-1,4-dihydroquinoline-2-carboxamide (**I-2**): White solid, yield 43%, m.p. 283–284°C. ¹H NMR (CD₂Cl₂ + CD₃OD + DMSO-*d*₆, 500 MHz) δ 8.63 – 8.57 (1H, m, Ph-H), 8.00 – 7.96 (1H, m, Ph-H), 7.62 – 7.56 (1H, m, Ph-H), 7.44 – 7.36 (2H, m, Ph-H and quinolone-H), 7.35 – 7.29 (1H, m, Ph-H), 4.11 (3H, s, OCH₃), 2.84 (3H, s, Ph-CH₃). ¹³C NMR (CD₂Cl₂ + CD₃OD + DMSO-*d*₆, 126 MHz) δ 161.2, 159.1, 158.7, 154.2, 148.3, 141.4, 132.9, 132.7, 128.4, 125.6, 124.2, 120.8, 118.9, 110.5, 104.7, 56.3, 23.1. HRMS (ESI⁺) *m/z* calcd for C₁₈H₁₅Cl₂N₂O₃ 377.0454, found 377.0453 [M + H]⁺.

8-methoxy-5-methyl-4-oxo-*N*-(2-(trifluoromethyl)phenyl)-1,4-dihydroquinoline-2-carboxamide (**I-3**): White solid, yield 60%, m.p. 232–234°C. ¹H NMR (CDCl₃, 500 MHz) δ 9.79 (1H, s, NH), 9.72 (1H, s, CONH), 7.97 (1H, d, *J* = 8.1 Hz, Ph-H), 7.73 (1H, d, *J* = 7.8 Hz, Ph-H), 7.66 (1H, t, *J* = 7.7 Hz, Ph-H), 7.42 (1H, t, *J* = 7.7 Hz, Ph-H), 7.13 (1H, d, *J* = 2.1 Hz, Ph-H), 6.92 (2H, s, quinolone-H and Ph-H), 3.98 (3H, s, OCH₃), 2.57 (3H, s, CH₃). ¹³C NMR (CDCl₃, 126 MHz) δ 181.8, 160.9, 146.5, 137.7, 134.1, 132.9, 131.9, 131.5, 127.4, 126.8, 126.6 (q, *J* = 5.0 Hz), 125.6, 124.9, 124.3 (q, *J* = 30.4 Hz), 123.7 (q, *J* = 273.9 Hz), 110.7, 109.3, 56.0, 22.1. HRMS (ESI⁺) *m/z* calcd C₁₉H₁₆F₃N₂O₃ for 377.1108, found 377.1109 [M + H]⁺.

8-methoxy-*N*-(2-methoxy-5-methylphenyl)-5-methyl-4-oxo-1,4-dihydroquinoline-2-carboxamide (**I-4**): White solid, yield 51%, m.p. 211–212°C. ¹H NMR (CD₂Cl₂, 500 MHz) δ 9.71 (1H, s, quinolone-NH), 8.87 (1H, s, CONH), 8.29 (1H, d, *J* = 1.8 Hz, Ph-H), 7.01 (2H, s, Ph-H), 6.99 (1H, dd, *J* = 8.3, 1.4 Hz, Ph-H), 6.89 (1H, d, *J*

= 8.3 Hz, Ph-H), 6.64 (1H, s, quinolone-H), 4.04 (3H, s, OCH₃), 3.95 (3H, s, OCH₃), 2.83 (3H, s, Ph-CH₃), 2.37 (3H, s, Ph-CH₃). ¹³C NMR (CD₂Cl₂, 126 MHz) δ 181.0, 159.0, 146.5, 138.0, 131.8, 131.1, 130.5, 129.8, 126.1, 125.4, 125.3, 120.5, 110.6, 110.1, 108.4, 100.9, 56.1, 55.9, 22.2, 20.7. HRMS (ESI⁺) m/z calcd for C₂₀H₂₁N₂O₄ 353.1496, found 353.1495 [M + H]⁺.

N-(3-isopropoxyphenyl)-8-methoxy-5-methyl-4-oxo-1,4-dihydroquinoline-2-carboxamide (**I-5**): White solid, yield 44%, m.p. 252–254°C. ¹H NMR (CD₂Cl₂ + CD₃OD, 500 MHz) δ 7.43 (1H, s, Ph-H), 7.30 – 7.29 (2H, m, Ph-H), 7.10 (1H, d, *J* = 8.1 Hz, Ph-H), 7.07 (1H, d, *J* = 8.4 Hz, Ph-H), 6.95 (1H, s, quinolone-H), 6.80 – 6.74 (1H, m, Ph-H), 4.64 – 4.61 (1H, m, CH), 4.05 (3H, s, OCH₃), 2.82 (3H, s, Ph-CH₃), 1.36 (6H, d, *J* = 6.1 Hz, (CH₃)₂). ¹³C NMR (CD₂Cl₂ + CD₃OD, 126 MHz) δ 158.3, 146.7, 129.5, 125.8, 113.3, 112.9, 112.5, 110.9, 110.8, 108.8, 108.6, 70.1, 55.8, 21.9, 21.4. HRMS (ESI⁺) m/z calcd for C₂₁H₂₃N₂O₄ 367.1652, found 367.1652 [M + H]⁺.

N-(2,4-dimethoxybenzyl)-8-methoxy-5-methyl-4-oxo-1,4-dihydroquinoline-2-carboxamide (**I-6**): White solid, yield 40%, m.p. 257–258°C. ¹H NMR (CD₂Cl₂ + CD₃OD, 500 MHz) δ 7.23 (1H, d, *J* = 8.3 Hz, Ph-H), 7.03 (2H, s, Ph-H), 6.68 (1H, s, quinolone-H), 6.51 (1H, d, *J* = 2.3 Hz, Ph-H), 6.47 (1H, dd, *J* = 8.3, 2.3 Hz, Ph-H), 4.55 (2H, s, CH₂), 4.01 (3H, s, OCH₃), 3.86 (3H, s, OCH₃), 3.80 (3H, s, OCH₃), 2.79 (3H, s, Ph-CH₃). ¹³C NMR (CD₂Cl₂ + CD₃OD, 126 MHz) δ 184.5, 163.3, 162.7, 160.6, 148.6, 140.6, 133.6, 132.8, 131.9, 127.7, 126.3, 119.7, 112.8, 110.1, 106.0, 100.3, 57.9, 57.1, 57.1, 41.2, 24.0. HRMS (ESI⁺) m/z calcd for C₂₁H₂₃N₂O₅ 383.1601, found 383.1600 [M + H]⁺.

8-methoxy-5-methyl-4-oxo-*N*-(3-(trifluoromethyl)benzyl)-1,4-dihydroquinoline-2-carboxamide (**I-7**): White solid, yield 41%, m.p. 214–215°C. ¹H NMR (CD₂Cl₂ + CD₃OD, 500 MHz) δ 8.11 (1H, s, NH), 7.66 (1H, s, Ph-H), 7.62 (1H, d, *J* = 7.7 Hz, Ph-H), 7.58 (1H, d, *J* = 7.8 Hz, Ph-H), 7.52 (1H, t, *J* = 7.8 Hz, Ph-H), 7.06 (2H, s, Ph-H), 6.73 (1H, s, quinolone-H), 4.68 (2H, s, CH₂), 4.03 (3H, s, OCH₃), 2.80 (3H, s, Ph-CH₃). ¹³C NMR (CD₃OD, 126 MHz) δ 181.9, 161.1, 146.0, 138.5, 137.9, 130.6, 130.2, 128.5, 125.2, 123.8, 123.6, 110.3, 107.6, 55.4, 42.8, 21.4. HRMS (ESI⁺) m/z calcd for C₂₀H₁₈F₃N₂O₃ 391.1264, found 391.1261 [M + H]⁺.

8-methoxy-5-methyl-4-oxo-*N*-(3',4',5'-trifluoro-[1,1'-biphenyl]-4-yl)-1,4-dihydroquinoline-2-carboxamide (**I-8**): White solid, yield 39%, m.p. 233–234°C. ¹H NMR (CD₂Cl₂, 500 MHz) δ 10.13 (1H, s, quinolone-NH), 9.66 (1H, s, CONH), 7.67 (1H, d, *J* = 7.8 Hz, Ph-H), 7.42 (1H, t, *J* = 7.4 Hz, Ph-H), 7.35 (1H, t, *J* = 7.5 Hz, Ph-H), 7.31 (1H, d, *J* = 7.4 Hz, Ph-H), 7.09 (1H, s, quinolone-H), 7.04 (2H, dd, *J* = 8.1, 6.8 Hz, Ph-H), 6.88 (1H, d, *J* = 8.0 Hz, Ph-H), 6.84 (1H, d, *J* = 8.1 Hz, Ph-H), 3.90 (3H, s, OCH₃), 2.37 (3H, s, Ph-CH₃). ¹³C NMR (CD₂Cl₂, 126 MHz) δ 181.0, 159.8, 145.9, 137.4, 134.5, 132.8, 131.1, 130.1, 129.5, 128.4, 126.7, 126.4, 124.8, 123.9, 112.5 (d, *J* = 5.3 Hz), 112.4 (d, *J* = 4.9 Hz), 110.0, 108.2, 55.3, 21.2. HRMS (ESI⁺) m/z calcd for C₂₄H₁₈F₃N₂O₃ 439.1264, found 439.1265 [M + H]⁺.

N-(4'-chloro-[1,1'-biphenyl]-4-yl)-8-methoxy-5-methyl-4-oxo-1,4-dihydroquinoline-2-carboxamide (**I-9**): White solid, yield 40%, m.p. 170–171 °C. ¹H NMR (CD₂Cl₂, 500 MHz) δ 10.23 (1H, s, NH), 8.55 (1H, dd, *J* = 8.2, 0.7 Hz, Ph-H), 7.52 (1H, s, Ph-H), 7.47 – 7.44 (2H, m, Ph-H), 7.42 – 7.35 (4H, m, Ph-H and quinolone-H), 7.25 (1H, dd, *J* = 7.6, 1.6 Hz, Ph-H), 7.18 (1H, td, *J* = 7.5, 1.1 Hz, Ph-H), 7.02 (1H, d, *J* = 8.2 Hz, Ph-H), 3.84 (3H, s, OCH₃), 2.73 (3H, s, Ph-CH₃). ¹³C NMR (CD₂Cl₂, 126 MHz) δ 160.7, 159.7, 158.3, 154.3, 148.8, 141.7, 136.6, 134.5, 133.7, 132.8, 131.4, 131.0, 130.6, 129.3, 128.7, 124.7, 124.3, 120.6, 120.4, 110.3, 103.4, 56.2, 23.2. HRMS (ESI⁺) *m/z* calcd for C₂₄H₂₀ClN₂O₃ 419.1157, found 419.1160 [M + H]⁺.

4.2.2 Synthetic procedure for II-1–II-13

2-(4-(2-fluorobenzoyl)piperazine-1-carbonyl)-8-methoxy-5-methylquinolin-4(1*H*)-one (**II-1**) was synthesized referring to the reported procedures.^[19] A mixture of 2-fluorobenzoic acid (0.28 g, 2.0 mmol), EDCl (0.45 g, 2.3 mmol) and HOBt (0.31 g, 2.3 mmol) in DMF (10 mL) was stirred for 30 min, followed by the addition of 8-methoxy-5-methyl-2-(piperazine-1-carbonyl)quinolin-4(1*H*)-one (0.50 g, 1.6 mmol). The solution was reacted for 12h, and then poured into DCM (100 mL). The organic phase was washed with water (100 mL), and separated by extraction. The resulting organic layer was dried, filtered and concentrated. The obtained residue was purified by chromatograph on silica gel using DCM/methanol (v/v = 100/1) as eluent to obtain **II-1**. Compounds **II-2** – **II-13** were provided in a similar manner.

2-(4-(2-fluorobenzoyl)piperazine-1-carbonyl)-8-methoxy-5-methylquinolin-4(1*H*)-one (**II-1**): White solid, yield 55%, m.p. 208–209 °C. ¹H NMR (CDCl₃, 500 MHz) δ 9.17 (1H, s, NH), 7.48 – 7.40 (2H, m, Ph-H), 7.24 (1H, t, *J* = 7.5 Hz, Ph-H), 7.12 (1H, t, *J* = 8.9 Hz, Ph-H), 6.96 (1H, d, *J* = 8.2 Hz, Ph-H), 6.92 (1H, d, *J* = 8.1 Hz, Ph-H), 6.25 (1H, s, quinolone-H), 3.95 (3H, s, OCH₃), 3.87 (4H, s, (CH₂)₂), 3.76 (2H, s, CH₂), 3.44 (2H, s, CH₂), 2.82 (3H, s, Ph-CH₃). ¹³C NMR (CDCl₃, 126 MHz) δ 180.5, 165.4, 164.4, 159.1, 157.1, 146.1, 138.4, 132.0 (d, *J* = 8.2 Hz), 131.8 (d, *J* = 58.3 Hz), 129.4 (d, *J* = 3.4 Hz), 125.4, 125.0 (d, *J* = 3.4 Hz), 124.6, 123.2 (d, *J* = 17.5 Hz), 115.9 (d, *J* = 21.4 Hz), 111.5, 110.6, 56.0, 46.8, 42.0, 22.5. HRMS (ESI⁺) *m/z* calcd for C₂₃H₂₃FN₃O₄ 424.1667, found 424.1671 [M + H]⁺.

8-methoxy-5-methyl-2-(4-(2-(trifluoromethyl)benzoyl)piperazine-1-carbonyl)quinolin-4(1*H*)-one (**II-2**): White solid, yield 60%, m.p. 255–257 °C. ¹H NMR (CDCl₃, 500 MHz) δ 9.28 (1H, s, NH), 7.72 (1H, d, *J* = 7.8 Hz, Ph-H), 7.63 (1H, t, *J* = 7.5 Hz, Ph-H), 7.55 (1H, t, *J* = 7.7 Hz, Ph-H), 7.34 (1H, d, *J* = 7.5 Hz, Ph-H), 6.95 (1H, d, *J* = 8.1 Hz, Ph-H), 6.91 (1H, d, *J* = 8.1 Hz, Ph-H), 6.23 (1H, s, quinolone-H), 4.07 – 3.97 (1H, m, piperazine-H), 3.96 – 3.87 (4H, m, OCH₃ and piperazine-H), 3.82 – 3.67 (3H, m, piperazine-H), 3.65 – 3.57 (1H, m, piperazine-H), 3.27 (2H, s, piperazine-CH₂), 2.81 (3H, s, Ph-CH₃). ¹³C NMR (CDCl₃, 126 MHz) δ 180.5, 167.6, 164.3, 146.2, 138.6, 134.0, 132.4, 132.1, 131.5, 129.6, 127.2, 126.9 (q, *J* = 32.0 Hz), 126.9 (q, *J* = 4.8 Hz), 125.5, 124.5, 123.6 (q, *J* = 274.2 Hz), 111.3, 110.6, 56.0, 46.8, 41.6, 22.5. HRMS (ESI⁺) *m/z* calcd for C₂₄H₂₃F₃N₃O₄ 474.1635, found 474.1638 [M + H]⁺.

2-(4-(2-chloro-4-(methylsulfonyl)benzoyl)piperazine-1-carbonyl)-8-methoxy-5-methylquinolin-4(1*H*)-one (**II-3**): White solid, yield 53%, m.p. 284–286 °C. ¹H NMR (DMSO-*d*₆, 500 MHz) δ 11.22 and 11.18 (1H, s, NH),

8.12 and 8.07 (1H, s, Ph-H), 8.01 and 7.96 (1H, d, $J=7.5$ Hz, Ph-H), 7.76 and 7.72 (1H, d, $J=7.5$ Hz, Ph-H), 7.14 and 7.11 (1H, d, $J=7.5$ Hz, Ph-H), 6.97 and 6.94 (1H, d, $J=7.5$ Hz, Ph-H), 5.99 and 5.95 (1H, s, quinolone-H), 3.97 and 3.94 (3H, s, OCH₃), 3.90 – 3.42 (6H, m, piperazine-CH₂), 3.34 – 3.15 (5H, m, SO₂CH₃ and piperazine-CH₂), 2.73 and 2.69 (3H, s, Ph-CH₃). ¹³C NMR (DMSO-*d*₆, 126 MHz) δ 179.0, 164.4, 162.7, 146.7, 143.2, 142.6, 140.1, 131.9, 130.1, 129.7, 129.1, 128.0, 126.3, 124.9, 124.0, 111.0, 108.4, 56.0, 46.6, 46.1, 45.9, 45.3, 43.1, 41.4, 41.0, 40.9, 40.4, 22.4. HRMS (ESI⁺) m/z calcd for C₂₄H₂₅ClN₃O₆S 518.1147, found 518.1151 [M + H]⁺.

8-methoxy-5-methyl-2-(4-(2-methylbenzoyl)piperazine-1-carbonyl)quinolin-4(1*H*)-one (**II-4**): White solid, yield 60%, m.p. 213–214°C. ¹H NMR (DMSO-*d*₆, 500 MHz) δ 11.23 and 11.16 (1H, s, NH), 7.37 – 7.09 (5H, m, Ph-H), 6.96 (1H, d, $J=7.9$ Hz, Ph-H), 5.96 and 5.91 (1H, s, quinolone-H), 3.96 and 3.93 (3H, s, OCH₃), 3.78 (1H, s, CH_AH_B), 3.69 (2H, s, CH₂), 3.53 (1H, s, CH_AH_B), 3.43 (1H, s, CH_AH_B), 3.27 (2H, s, CH₂), 3.17 (1H, s, CH_AH_B), 2.71 and 2.67 (3H, s, Ph-CH₃), 2.24 and 2.22 (3H, s, Ph-CH₃). ¹³C NMR (DMSO-*d*₆, 126 MHz) δ 179.6, 169.3, 163.3, 147.3, 143.9, 139.7, 136.5, 134.24, 132.4, 130.7, 130.1, 129.3, 126.2, 125.4, 124.6, 111.6, 108.9, 56.6, 47.3, 46.9, 46.5, 45.9, 42.1, 41.6, 41.2, 23.0, 19.1. HRMS (ESI⁺) m/z calcd for C₂₄H₂₆N₃O₄ 420.1918, found 420.1917 [M + H]⁺.

8-methoxy-2-(4-(2-methoxybenzoyl)piperazine-1-carbonyl)-5-methylquinolin-4(1*H*)-one (**II-5**): White solid, yield 62%, m.p. 241–242°C. ¹H NMR (DMSO-*d*₆, 500 MHz) δ 11.24 and 11.19 (1H, s, NH), 7.43 and 7.37 (1H, t, $J=7.5$ Hz, Ph-H), 7.23 and 7.20 (1H, d, $J=7.0$ Hz, Ph-H), 7.16 – 6.92 (4H, m, Ph-H), 5.97 and 5.93 (1H, s, quinolone-H), 3.96 and 3.93 (3H, s, OCH₃), 3.83 and 3.78 (3H, s, OCH₃), 3.73 – 3.51 (4H, m, piperazine-CH₂), 3.41 (1H, s, piperazine-CH₂), 3.33 – 3.08 (3H, m, piperazine-CH₂), 2.72 and 2.68 (3H, s, Ph-CH₃). ¹³C NMR (DMSO-*d*₆, 126 MHz) δ 179.6, 167.1, 163.2, 147.3, 143.9, 140.1, 135.1, 132.4, 131.0, 130.2, 129.3, 128.3, 125.7, 124.6, 121.2, 111.9, 108.9, 56.6, 56.0, 47.3, 46.9, 46.6, 45.9, 42.1, 41.7, 41.4, 40.8, 23.0. HRMS (ESI⁺) m/z calcd for C₂₄H₂₆N₃O₅ 436.1867, found 436.1866 [M + H]⁺.

8-methoxy-5-methyl-2-(4-(2-methyl-4-(trifluoromethyl)thiazole-5-carbonyl)piperazine-1-carbonyl)quinolin-4(1*H*)-one (**II-6**): White solid, yield 66%, m.p. 225–257°C. ¹H NMR (CDCl₃, 500 MHz) δ 9.34 (1H, s, NH), 6.96 (1H, d, $J=8.2$ Hz, Ph-H), 6.92 (1H, d, $J=8.1$ Hz, Ph-H), 6.24 (1H, s, quinolone-H), 3.93 (3H, s, OCH₃), 3.90 – 3.69 (6H, m, piperazine-CH₂), 3.43 (2H, s, piperazine-CH₂), 2.81 (3H, s, thiazole-CH₃), 2.77 (3H, s, Ph-CH₃). ¹³C NMR (CDCl₃, 126 MHz) δ 180.49, 168.39, 164.38, 159.51, 146.18, 139.90 (q, $J=36.7$ Hz), 138.5, 132.1, 131.5, 131.0, 125.5, 124.6, 120.1 (q, $J=272.4$ Hz), 111.3, 110.7, 56.0, 47.1, 42.2, 22.5, 19.1. HRMS (ESI⁺) m/z calcd for C₂₂H₂₂F₃N₄O₄S 495.1308, found 495.1311 [M + H]⁺.

8-methoxy-5-methyl-2-(4-(4-methyl-1,2,3-thiadiazole-5-carbonyl)piperazine-1-carbonyl)quinolin-4(1*H*)-one (**II-7**): White solid, yield 64%, m.p. 211–213°C. ¹H NMR (CDCl₃, 500 MHz) δ 9.29 (1H, s, NH), 6.97 (1H, d, $J=8.2$ Hz, Ph-H), 6.93 (1H, d, $J=8.1$ Hz, Ph-H), 6.24 (1H, s, quinolone-H), 3.94 (3H, s, OCH₃), 3.90 – 3.15 (8H, m, piperazine-CH₂), 2.81 (3H, s, Ph-CH₃), 2.74 (3H, s, thiadiazole-CH₃). ¹³C NMR (CDCl₃, 126 MHz) δ

180.5, 164.4, 160.5, 157.5, 146.2, 141.7, 138.3, 132.1, 131.5, 125.6, 124.6, 111.4, 110.7, 56.0, 46.8, 42.5, 22.5, 13.0. HRMS (ESI⁺) m/z calcd for C₂₀H₂₂N₅O₄S 428.1387, found 428.1389 [M + H]⁺.

2-(4-(3,4-dichloroisothiazole-5-carbonyl)piperazine-1-carbonyl)-8-methoxy-5-methylquinolin-4(1*H*)-one (**II-8**): White solid, yield 58%, m.p. 185–186°C. ¹H NMR (CDCl₃, 500 MHz) δ 9.35 (1H, s, NH), 6.97 (1H, d, *J* = 8.2 Hz, Ph-H), 6.93 (1H, d, *J* = 8.1 Hz, Ph-H), 6.25 (1H, s, quinolone-H), 3.93 (3H, s, OCH₃), 3.90 – 3.35 (8H, m, (CH₂)₄), 2.81 (3H, s, Ph-CH₃). ¹³C NMR (CDCl₃, 126 MHz) δ 180.5, 164.4, 158.7, 154.5, 148.5, 146.2, 138.5, 132.1, 131.5, 125.6, 124.6, 120.5, 111.3, 110.7, 56.0, 46.9, 42.5, 22.5. HRMS (ESI⁺) m/z calcd for C₂₀H₁₉Cl₂N₄O₄S 481.0499, found 481.0501 [M + H]⁺.

2-(4-(4-chloro-3-ethyl-1-methyl-1*H*-pyrazole-5-carbonyl)piperazine-1-carbonyl)-8-methoxy-5-methylquinolin-4(1*H*)-one (**II-9**): White solid, yield 57%, m.p. 186–187°C. ¹H NMR (DMSO-*d*₆, 500 MHz) δ 11.30 – 11.15 (1H, s, NH), 7.13 (1H, s, Ph-H), 6.96 (1H, s, Ph-H), 5.98 (1H, s, quinolone-H), 3.96 (3H, s, OCH₃), 3.85 – 3.65 (7H, m, pyrazole-CH₃ and (CH₂)₂), 3.58 – 3.39 (4H, m, (CH₂)₂), 2.72 (3H, s, Ph-CH₃), 2.65 – 2.52 (2H, m, CH₂CH₃), 1.25 – 1.13 (3H, m, CH₂CH₃). ¹³C NMR (DMSO-*d*₆, 126 MHz) δ 179.6, 163.3, 159.1, 148.8, 147.3, 143.7, 133.9, 132.4, 130.2, 125.4, 124.6, 111.6, 109.0, 105.8, 56.6, 47.6, 46.7, 46.1, 42.4, 42.0, 41.5, 38.5, 22.9, 19.0, 13.1. HRMS (ESI⁺) m/z calcd for C₂₃H₂₇ClN₅O₄ 472.1746, found 472.1746 [M + H]⁺.

8-methoxy-5-methyl-2-(4-(1-methyl-3-(trifluoromethyl)-1*H*-pyrazole-4-carbonyl)piperazine-1-carbonyl)quinolin-4(1*H*)-one (**II-10**): White solid, yield 60%, m.p. 221–222°C. ¹H NMR (DMSO-*d*₆, 500 MHz) δ 11.20 (1H, s, NH), 8.16 (1H, s, pyrazole-H), 7.13 (1H, d, *J* = 7.9 Hz, Ph-H), 6.96 (1H, d, *J* = 7.8 Hz, Ph-H), 5.96 (1H, s, quinolone-H), 3.95 (6H, s, OCH₃ and pyrazole-CH₃), 3.59 (6H, s, (CH₂)₃), 3.34 (2H, s, CH₂), 2.70 (3H, s, Ph-CH₃). ¹³C NMR (DMSO-*d*₆, 126 MHz) δ 179.6, 163.3, 161.6, 147.3, 143.8, 138.2 (q, *J* = 36.9 Hz), 133.0, 132.4, 130.2, 125.4, 124.6, 121.5 (q, *J* = 269.39 Hz), 115.2, 111.6, 109.0, 56.6, 47.0, 41.8, 22.9. HRMS (ESI⁺) m/z calcd for C₂₂H₂₃F₃N₅O₄ 478.1697, found 478.1694 [M + H]⁺.

2-(4-(3-(difluoromethyl)-1-methyl-1*H*-pyrazole-4-carbonyl)piperazine-1-carbonyl)-8-methoxy-5-methylquinolin-4(1*H*)-one (**II-11**): White solid, yield 62%, m.p. 201–203°C. ¹H NMR (DMSO-*d*₆, 500 MHz) δ 11.24 (1H, s, NH), 8.13 (1H, s, pyrazole-H), 7.13 (1H, d, *J* = 8.1 Hz, Ph-H), 7.07 (1H, t, *J* = 54.5 Hz, CHF₂), 6.97 (1H, d, *J* = 7.7 Hz, Ph-H), 5.97 (1H, s, quinolone-H), 3.95 (3H, s, OCH₃), 3.90 (3H, s, pyrazole-CH₃), 3.67 – 3.59 (6H, m, (CH₂)₃), 3.38 (2H, s, CH₂), 2.71 (3H, s, Ph-CH₃). ¹³C NMR (DMSO-*d*₆, 126 MHz) δ 179.6, 163.3, 162.4, 147.3, 144.3 (t, *J* = 25.3 Hz), 143.9, 132.7, 132.4, 130.2, 125.4, 124.6, 114.7, 111.5, 110.9 (t, *J* = 234.4 Hz), 109.0, 56.6, 47.0, 41.8, 39.5, 22.9. HRMS (ESI⁺) m/z calcd for C₂₂H₂₄F₂N₅O₄ 460.1791, found 460.1789 [M + H]⁺.

(*E*)-2,6-dimethoxy-4-(3-(4-(8-methoxy-5-methyl-4-oxo-1,4-dihydroquinoline-2-carbonyl)piperazin-1-yl)-3-oxoprop-1-en-1-yl)phenyl acetate (**II-12**): White solid, yield 55%, m.p. 173–174°C. ¹H NMR (CDCl₃, 500 MHz) δ 9.30 (1H, s, NH), 7.62 (1H, d, *J* = 15.3 Hz, CH), 6.96 (1H, d, *J* = 8.1 Hz, Ph-H), 6.92 (1H, d, *J* = 8.1 Hz,

Ph-H), 6.79 (1H, d, $J = 15.3$ Hz, CH), 6.76 (2H, s, Ph-H), 6.27 (1H, s, quinolone-H), 3.94 (3H, s, OCH₃), 3.84 (6H, s, OCH₃), 3.80 (8H, s, piperazine-CH₂), 2.82 (3H, s, COCH₃), 2.33 (3H, s, Ph-CH₃). ¹³C NMR (CDCl₃, 126 MHz) δ 180.6, 168.6, 165.5, 164.2, 152.4, 146.2, 143.7, 138.7, 133.2, 132.1, 131.5, 130.2, 125.5, 124.5, 116.5, 111.4, 110.7, 104.6, 56.3, 56.0, 45.4, 42.0, 22.5, 20.4. HRMS (ESI⁺) m/z calcd for C₂₉H₃₂N₃O₈ 550.2184, found 550.2188 [M + H]⁺.

(*E*)-6-methoxy-5-(6-(4-(8-methoxy-5-methyl-4-oxo-1,4-dihydroquinoline-2-carbonyl)piperazin-1-yl)-3-methyl-6-oxohex-2-en-1-yl)-7-methyl-3-oxo-1,3-dihydroisobenzofuran-4-yl acetate (**II-13**): White solid, yield 47%, m.p. 153–154°C. ¹H NMR (CDCl₃, 500 MHz) δ 9.16 (1H, s, NH), 6.97 (1H, d, $J = 8.1$ Hz, Ph-H), 6.93 (1H, d, $J = 8.1$ Hz, Ph-H), 6.25 (1H, s, quinolone-H), 5.16 (2H, s, isobenzofuran-1(3*H*)-one-CH₂), 5.07 (1H, t, $J = 6.4$ Hz, CH), 3.96 (3H, s, OCH₃), 3.80 (3H, s, OCH₃), 3.75 – 3.63 (6H, m, piperazine-CH₂), 3.52 (2H, s, piperazine-CH₂), 3.37 (2H, d, $J = 6.6$ Hz, Ph-CH₂), 2.82 (3H, s, Ph-CH₃), 2.43 – 2.37 (5H, m, COCH₃ and CH₂), 2.34 – 2.29 (2H, m, CH₂), 2.23 (3H, s, Ph-CH₃), 1.81 (3H, s, CH₃). ¹³C NMR (CDCl₃, 126 MHz) δ 180.6, 171.2, 169.0, 168.3, 164.3, 162.6, 146.3, 146.2, 145.9, 138.5, 134.9, 132.1, 131.6, 129.2, 125.5, 124.6, 123.0, 122.0, 113.5, 111.5, 110.7, 68.4, 61.3, 56.0, 45.4, 41.4, 34.4, 31.6, 23.5, 22.5, 20.6, 16.6, 11.8. HRMS (ESI⁺) m/z calcd for C₃₅H₄₀N₃O₉ 646.2759, found 646.2762 [M + H]⁺.

4.3 Fungicidal activity measurement

With fluopyram and carbendazim as positive controls, the mycelial growth inhibition method was used to determine the in vitro inhibitory activities of the target molecules against common agricultural pathogens according to the previously reported procedures.²² The tested pathogens include *Rhizoctonia solani* (RS), *Gibberella zea* (GZ), *Botrytis cinerea* (BC), *Physalospora piricola* (PP), *Cercospora circumscissa* Sacc. (CS), *Colletotrichum capsici* (CC), *Alternaria kikuchiana* Tanaka (AK), and *Alternaria* sp. (AS).

4.4 In vitro Cellular Cytotoxicity Assays

The in vitro cell viability of hepatocellular carcinoma cell lines (HepG-2) was assessed by MTT colorimetric assay according to the reported methods.^{23,24} Firstly, cells were seeded in 96-well plates, incubated in a CO₂ incubator at 37°C for 24 h, and then treated with freshly prepared culture mediums containing the tested compounds (100 μ M) for 24h. Secondly, a fresh solution of MTT (5 mg/ml) was added to each single well of the 96-well plate, which was further incubated in a CO₂ incubator for another 4 h. After removal of the medium, the cells were dissolved with 100 μ L of DMSO and analyzed in a multiwell-plate reader (Bio-Rad iMark) at 490 nm.

4.5 Fluorescence characteristics determination

4.5.1 Fluorescence characteristics measurement

The UV-Vis absorption spectra was firstly measured from 200 nm to 800 nm at 50 μ M to determine the appropriate excitation wavelength. The fluorescence emission spectra were provided with EM slit of 5 nm, PMT voltage of 480 V at the same concentration (50 μ M). Subsequently, the absolute fluorescence

quantum yields (QY) were recorded on a FLS1000 spectrometer with the parameters referred to the obtained fluorescence emission and excitation spectra.

4.5.2 TD-DFT calculation

The singlet ground-states geometrical optimizations were performed, and the calculations were carried out by using spin-restricted DFT method with B3LYP,²⁵⁻²⁸ in conjunction with 6-31+G(d,p) basis set. Based on the optimized geometries of the molecules, the molecular orbitals (MOs) were calculated at the same level. The HOMO energy (E_{HOMO}) of each compounds are taken from the eigenvalues of the Kohn-Sham calculated from the DFT. TD-DFT calculation of the single excitation energies were performed at the ground states and the calculations using B3LYP, and the basis set is 6-31+G(d,p). Then the energy gaps (E_g) were estimated based on the single-singlet electronic transition energies. The LUMO energy level (E_{LUMO}) can be got according the equation of $E_{\text{LUMO}}=E_{\text{HOMO}}(\text{DFT})+E_g(\text{TDDFT})$. The E_{LUMO} got from this way are excellent agreement with the experiments for the compounds.²⁹ All the calculations of both ground and excited states were performed within the Gaussian 09 quantum chemical package.^[30]

Declarations

Acknowledgments

This research was supported by the National Natural Science Foundation of China (No. 32001929), the National Innovation and Entrepreneurship Training Program for College Students (No. 202110447013, 202110447032), and the Innovation and Entrepreneurship Training Program for College Students of Liaocheng University (No. CXCY2020Y116).

Conflict of interest

There are no conflicts of interest to declare.

References

1. Kabbage M, Piotrowski JS, Thill E, Westrick NM, Ralph J, Hockemeyer K, Koch PL (2020) *Plant Pathol* 69:112
2. Zhu JK, Gao JM, Yang CJ, Shang XF, Zhao ZM, Lawoe RK, Zhou R, Sun Y, Yin XD, Liu YQ (2020) *J Agric Food Chem* 68:2306
3. Zheng JG, Liu TT, Guo ZX, Zhang L, Mao LG, Zhang YN, Jiang HY (2019) *Sci Rep-UK* 9:1
4. Song PP, Zhao J, Liu ZL, Duan YB, Hou YP, Zhao CQ, Wu M, Wei M, Wang NH, Lv Y, Han ZJ (2017) *Pest Manag Sci* 73:94
5. Zhang ZL, Xie YJ, Hu X, Shi HA, Wei M, Lin ZF (2018) *Nat Prod Commun* 13:1721
6. Hasheminejad N, Khodaiyan F, Safari M (2019) *Food Chem* 275:113

7. Yang GZ, Zhu JK, Yin XD, Yan YF, Wang YL, Shang XF, Liu YQ, Zhao ZM, Peng JW, Liu H (2019) *J Agric Food Chem* 67:11340
8. Li JW, Vederas JC (2009) *Science* 325:161
9. Rodrigues T, Reker D, Petra Schneider P, Schneider G (2016) *Nat Chem* 8:531
10. Newman DJ, Cragg GM (2020) *J Nat Prod* 83:770
11. Liu J, Lu SC, Feng JY, Li CK, Wang WL, Pei YM, Ding SL, Zhang M, Li HL, Na RS, Li QX (2020) *J Agric Food Chem* 68:2116
12. Jadulco RC, Pond CD, Van Wagoner RM, Koch M, Gideon OG, Matainaho TK, Piskaut P, Barrows LR (2014) *J Nat Prod* 77:183
13. Cretton S, Dorsaz S, Azzollini A, Favre-Godal Q, Marcourt L, Ebrahimi SN, Voinesco F, Michellod E, Sanglard D, Gindro K, Wolfender JL, Cuendet M, Christen P (2016) *J Nat Prod* 79:300
14. Dorsaz S, Snäkä T, Favre-Godal Q, Maudens P, Boulens N, Furrer P, Ebrahimi SN, Hamburger M, Allémann E, Gindro K, Queiroz EF, Riezman H, Wolfender JL, Sanglard D (2017) *Antimicrob. Agents Ch.* 61, e00829-17/1
15. Hua XW, Liu WR, Chen Y, Ru J, Guo SJ, Yu XB, Cui YH, Liu XH, Gu YC, Xue CM, Liu Y, Sui JK, Wang GQ (2021) *J Agric Food Chem* 69:11470
16. Hua X, Liu N, Zhou S, Zhang L, Yin H, Wang G, Fan Z, Ma Y (2020) *Engineering* 6:553
17. Hua X, Liu N, Fan Z, Zong G, Ma Y, Lei K, Yin H, Wang G (2019) *Chin J Org Chem* 39:2581
18. Hua X, Liu W, Su Y, Liu X, Liu J, Liu N, Wang G, Jiao X, Fan X, Xue C, Liu Y, Liu M (2020) *Pest Manag Sci* 76:2368
19. Liu WR, Hua XW, Zhou S, Yuan FY, Wang GQ, Liu Y, Xing XR (2021) *Chinese J Struct Chem* 40:666
20. Wang BL, Li ZM, Zhang Y, Zhang LY, Zhang X, Li YH (2017) *CN 105541748*,
21. Bink A, Govaert G, François I, Pellens K, Meerpoel L, Borgers M, Minnebruggen GV, Vroome V, Cammue B, Thevissen K (2010) *FEMS Yeast Res* 10:812
22. Fan ZJ, Yang ZK, Zhang HK, Mi N, Wang H, Cai F, Zuo X, Zheng QX, Song HB (2010) *J Agric Food Chem* 58:2630
23. An BH, Zhang RF, Li QL, Du XM, Ru J, Zhang SL, Ma CL (2019) *J Organomet Chem* 881:51
24. Li LM, Chen Y, Wang QP, Li ZJ, Liu ZF, Hua XW, Han J, Chang CX, Wang ZP, Li DC (2021) *Int J Nanomed* 16:5513
25. Beck AD (1993) *J Chem Phys* 98:1372
26. Beck AD (1993) *J Chem Phys* 98:5648
27. Yanai T, Tew DP, Handy NC (2004) *Chem Phys Lett* 393:51
28. Hertwing RH, Koch W (1997) *Chem Phys Lett* 268:345
29. Ku J, Lansac Y, Jang YH (2011) *J Phys Chem C* 115:21508
30. Frisch MJ, Trucks GW, Schlegel HB, Scuseria GE, Robb MA et al (2009) Gaussian, Inc., Wallingford CT,

Schemes 1

Schemes 1 is available in the Supplemental Files section

Figures

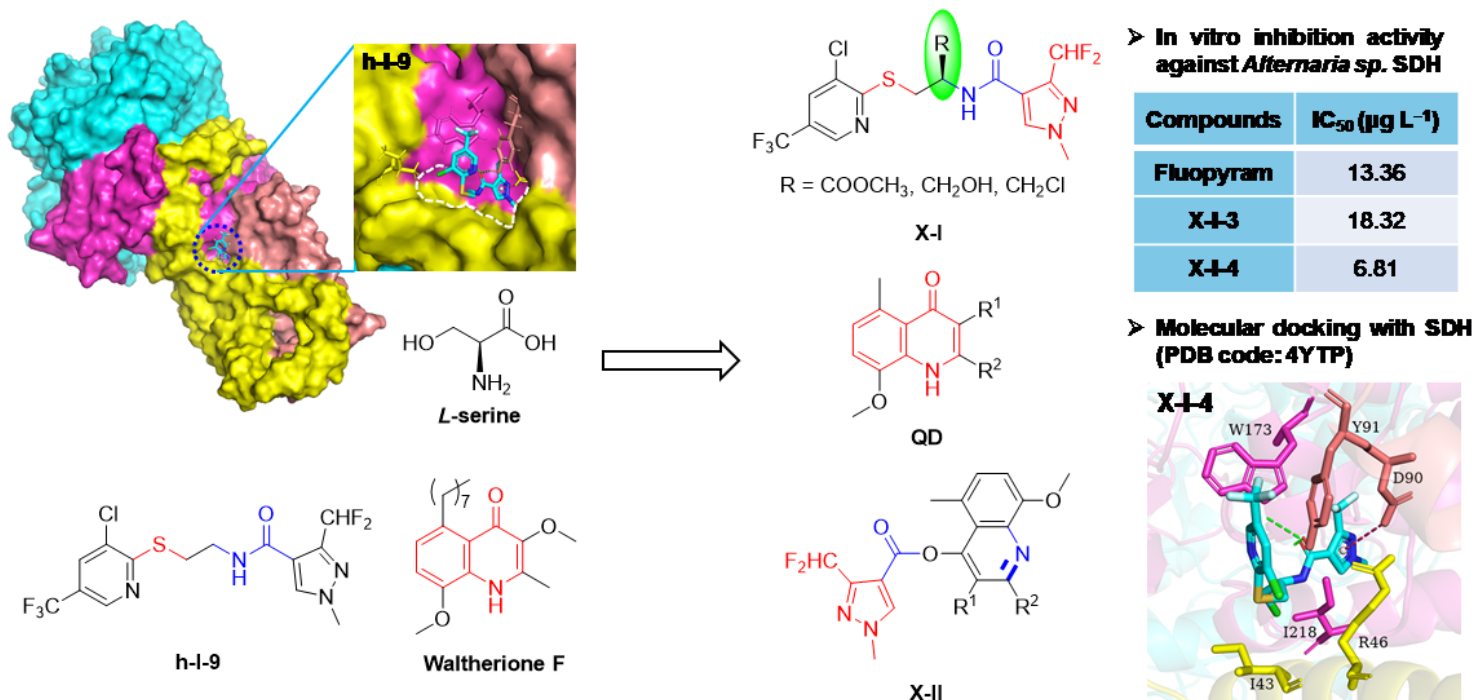


Figure 1

The molecules obtained in the previous work

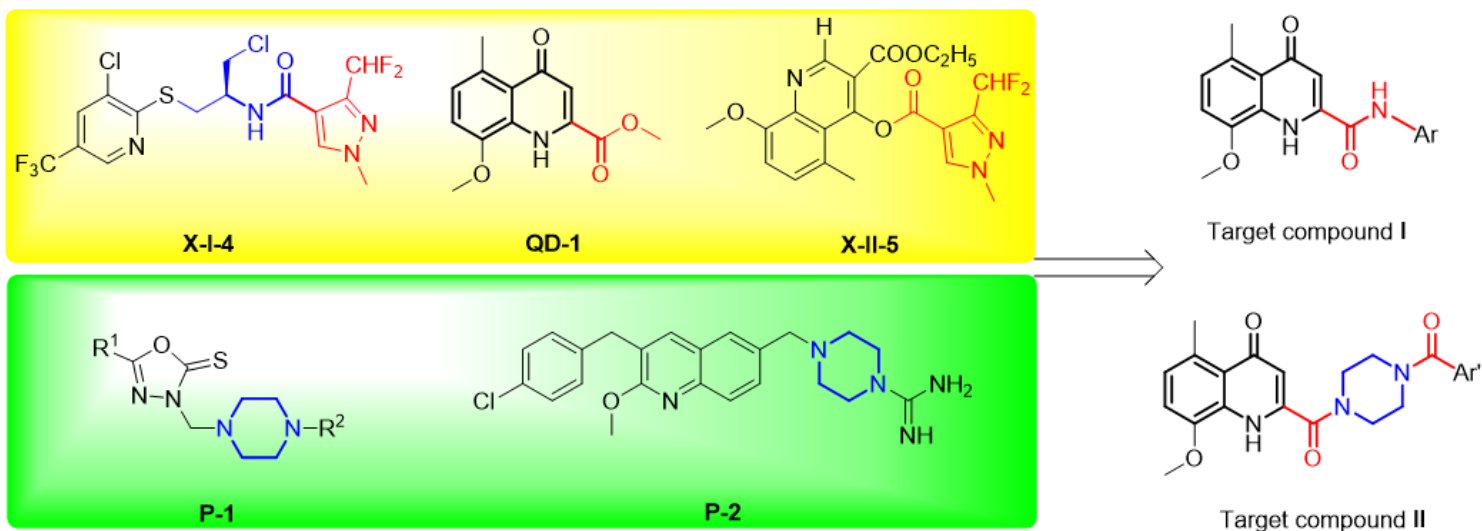


Figure 2

Molecular design strategy in this project

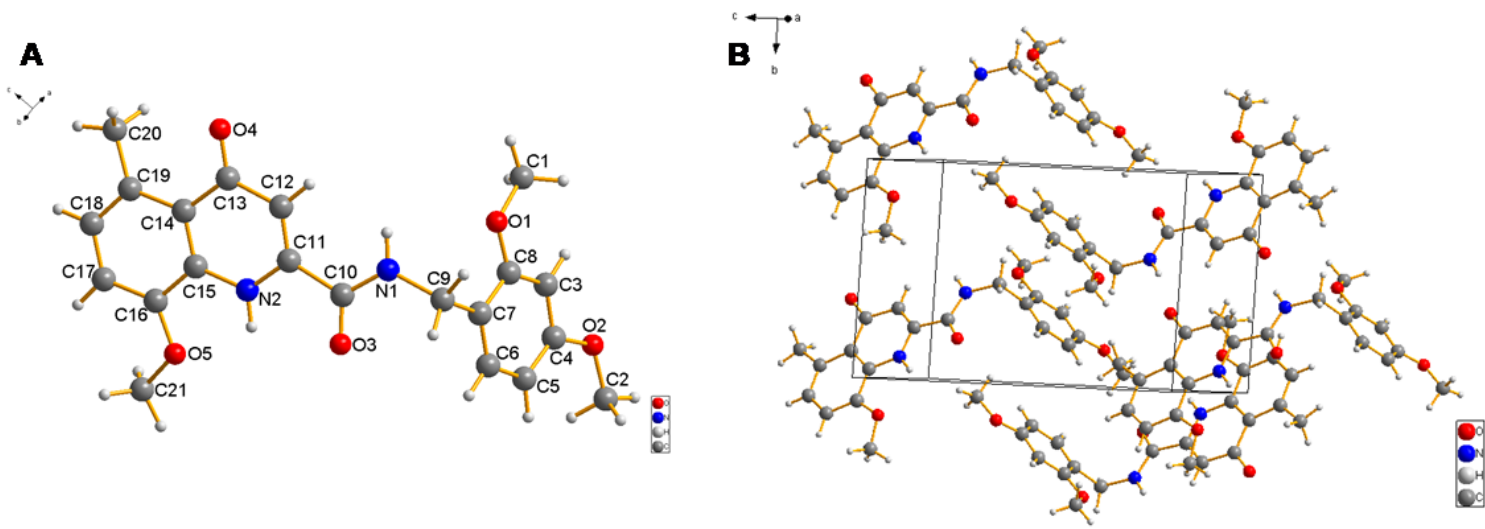


Figure 3

The crystal structure (A) and packing (B) of the target compound I-6

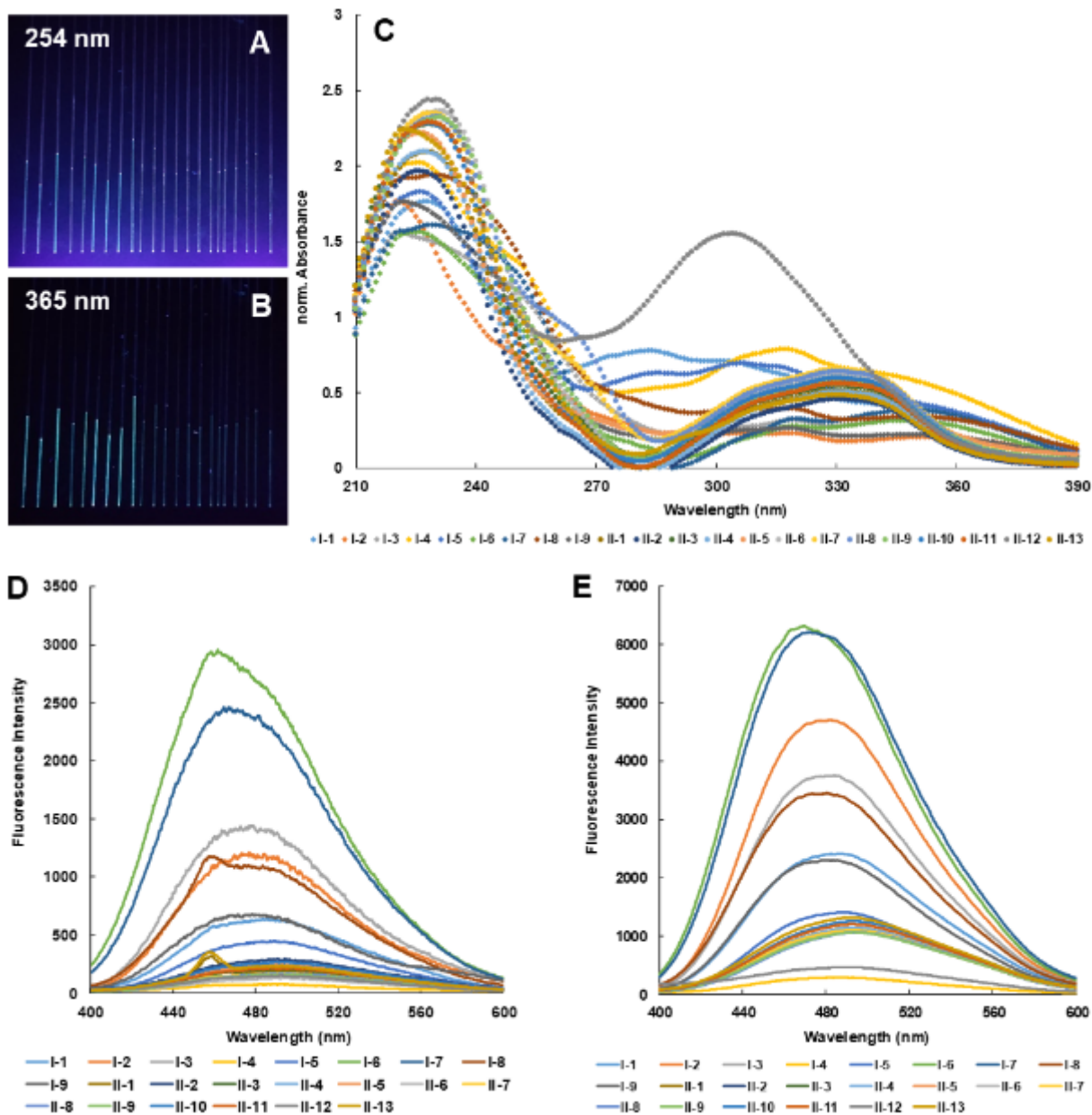


Figure 4

Methanol solutions (50 μM) of the target compounds I-1 – I-9 and II-1 – II-13 under 254 nm (A) and 365 nm (B) light irradiation, and UV-Vis absorption spectra (C), and fluorescence emission spectra at the first (D) and second (E) excitation wavelengths

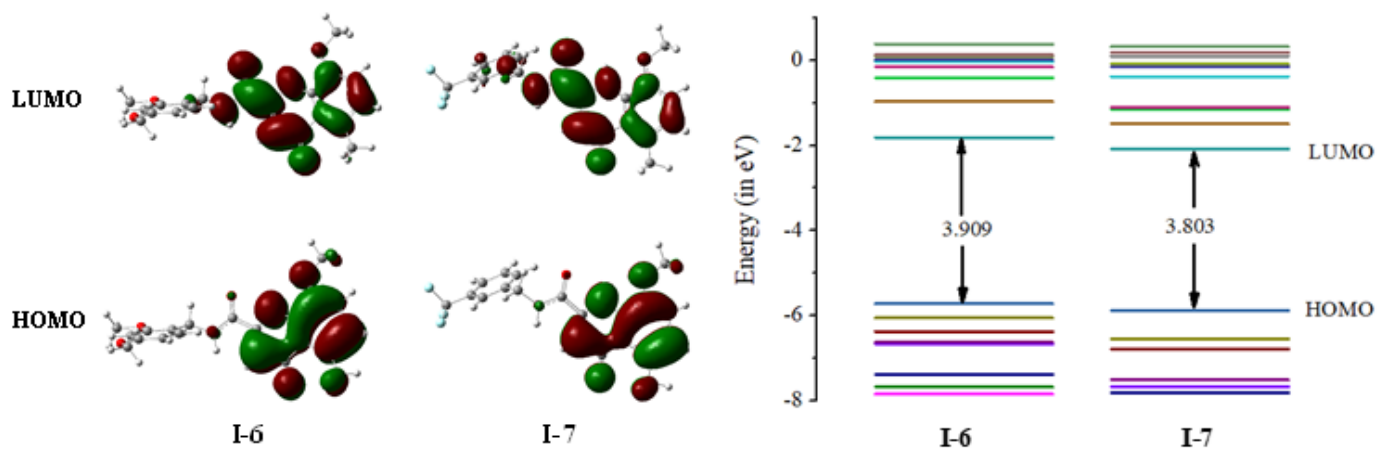


Figure 5

HOMO and LUMO orbitals of molecules I-6 and I-7.

Supplementary Files

This is a list of supplementary files associated with this preprint. Click to download.

- [Scheme1.png](#)
- [supportinginformation.docx](#)